Supplementary information for:

Sustained translational repression by eIF2α−P mediates prion neurodegeneration

Julie A. Moreno[1], Helois Radford[1], Diego Peretti[1], Joern R. Steinert[1], Nicholas Verity[1], Maria Guerra Martin[1], Mark Halliday[1], Jason Morgan[1], David Dinsdale[1], Catherine A. Ortori[2], David A. Barrett[2], Pavel Tsaytler[3], Anne Bertolotti[3], Anne E. Willis[1], Martin Bushell[1] and Giovanna R. Mallucci[1]*.

[1]MRC Toxicology Unit, Hodgkin Building, University of Leicester, Lancaster Road, Leicester LE1 9HN, UK
[2]Centre for Analytical Bioscience, School of Pharmacy, University of Nottingham, Nottingham NG7 2RD, UK
[3]MRC Laboratory of Molecular Biology, Hills Road, Cambridge CB2 0QH, UK.

*To whom correspondence should be addressed. E-mail: grm7@le.ac.uk

Supplementary Figures 1-10 and Legends
Supplementary methods
Supplementary references

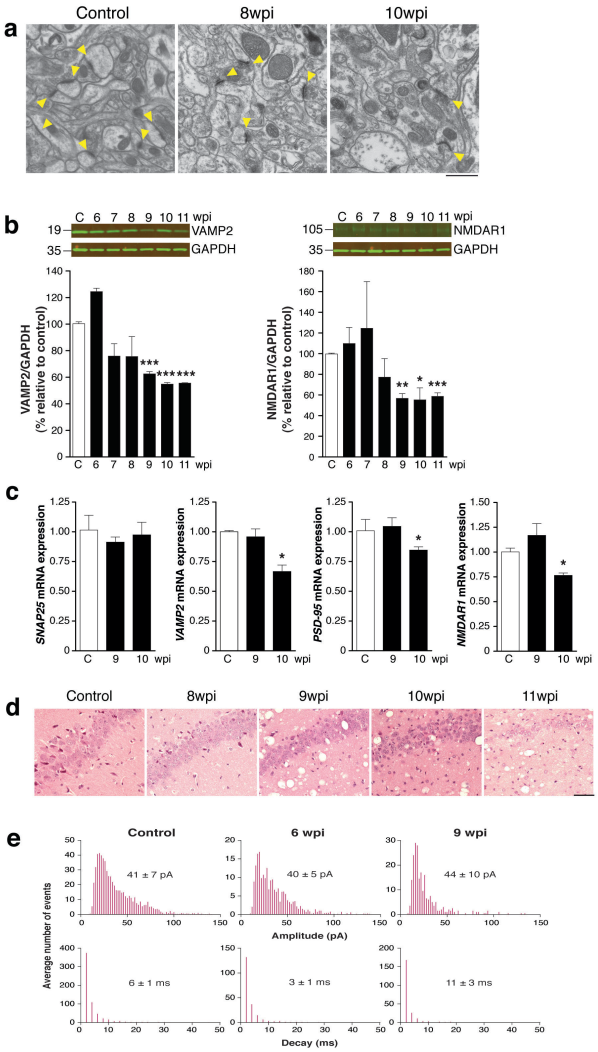

Figure S1. Synaptic changes in prion-infected mice.
a, Representative electron microscopic (EM) images of stratum radiatum of CA1 region of the hippocampus from prion-infected mice. Synapses (indicated by yellow arrowheads) are scored by the presence of synaptic vesicles pre-synaptically, a synaptic cleft and post-synaptic density (PSD). Scale bar: 2μm **b,** The synaptic proteins VAMP2 and NMDAR1 decline significantly at 9wpi in prion-infected mice. Representative western blots are shown. Bar graphs show quantitation compared to GAPDH loading control. **c,** qPCR data for *SNAP25, VAMP2, NMDAR1, PSD-95* mRNAs at 9 and 10wpi. There is no change in mRNA levels until 10wpi when neuronal numbers decline. n = 3 mice, repeated in triplicate. Bars represent mean ± s.e.m. One-way ANOVA with Tukey's post test was used for multiple comparisons; p <0.05*; p <0.005**, p <0.0001***. **d,** Haematoxylin and eosin (H&E) stained sections from prion-infected mice show evolution of spongiform change and neuronal loss throughout the course of prion disease. Scale bar: 50μm. **e,** Amplitude (top) and decay histograms (bottom) showing fewer events per recorded neuron from prion-infected mice, with unchanged mean amplitudes and decay kinetics from whole cell recordings. Control mice were injected with normal brain homogenate (NBH) and examined at each time point. Data from controls at all time points was averaged or a representative image is shown, due to lack variability over the time course, to simplify figures.

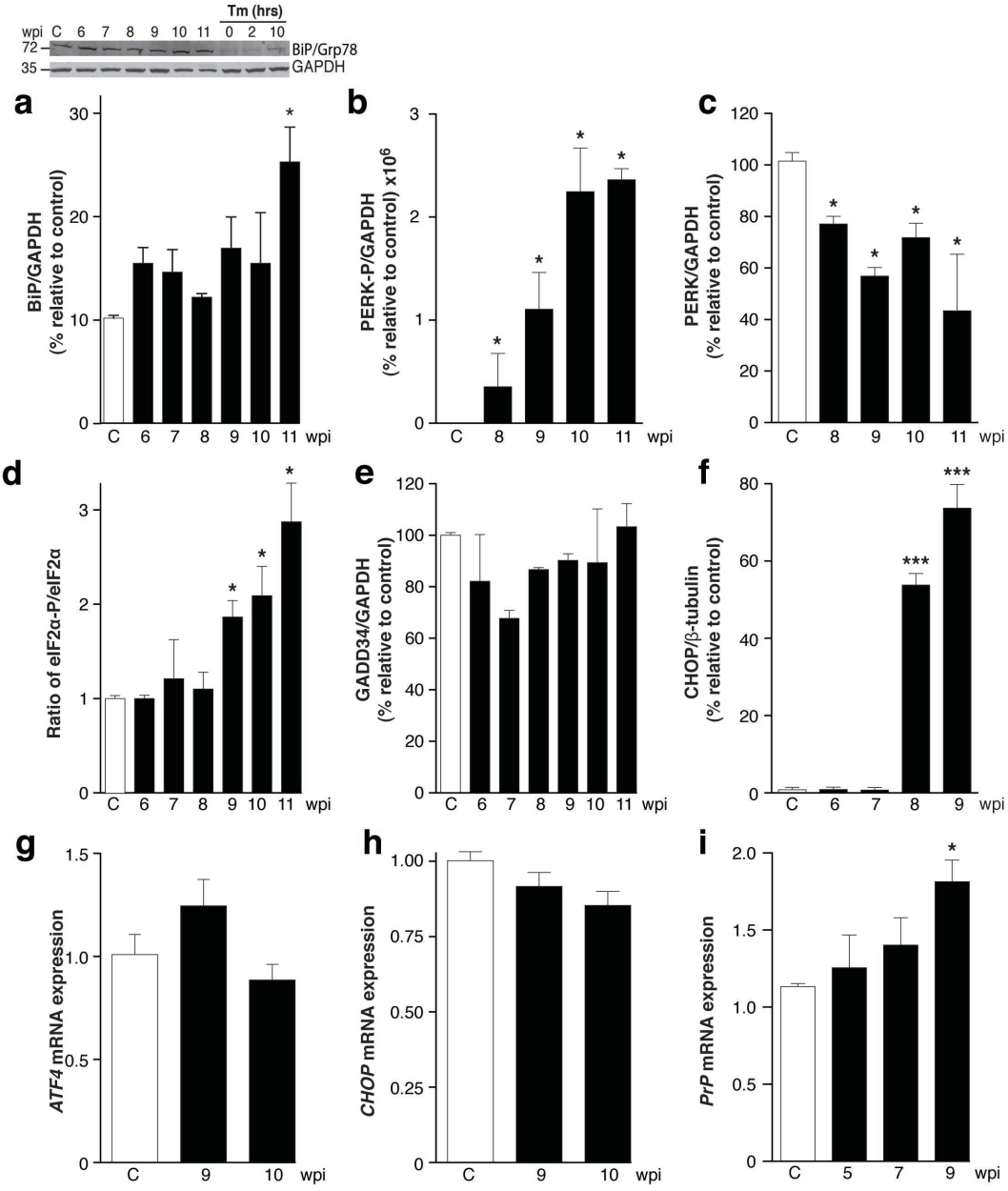

Figure S2. Quantification of proteins and mRNAs in the eIF2α translational repression pathway during prion disease. a, BiP levels rise modestly towards end-stage prion disease. Representative western blots and bar chart showing quantification. **b,** and **c**, PERK-P levels rise significantly as disease evolves, with corresponding decline in PERK. No PERK-P is detected in control mice. **d,** There is a significant rise eIF2α-P relative to eIF2α in prion-infected mice at 9wpi; **e**, GADD34 levels do not significantly change over the course of prion disease, but **f**, CHOP levels increase at 9wpi consistent with eIF2α-P activation. Controls are for 11wpi time point on western blots, n = 3 mice. **g-h**, qPCR results for *ATF4, CHOP* and *PrP* mRNAs. For all mRNA experiments n = 3 mice, repeated in triplicate. Data in bar charts represents mean ± s.e.m. One-way ANOVA with Tukey's post test was used for multiple comparisons; $p < 0.05$*; $p < 0.005$**.

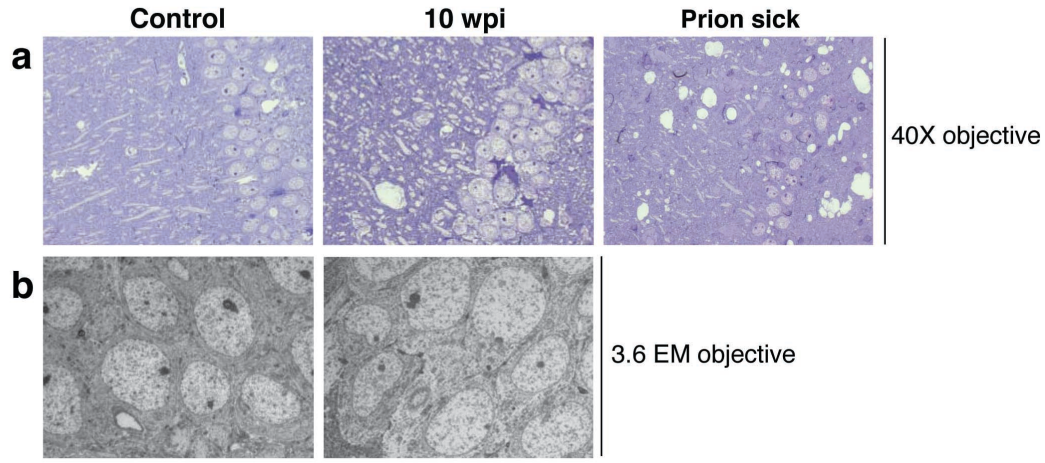

Figure S3. Cell death in prion disease. Swollen pyramidal neurons atypical of apoptosis, autophagy or necrosis are seen in prion-diseased mice. **a**, Semi-thin sections of stratum radiatum of CA1 region of the hippocampus from which EM images are taken show swollen and degenerating neurons at 10wpi and extensive neuronal loss in terminally ill mice. **b**, EM images of swollen neurons at 10wpi compared to controls, NBH injected mice at 10wpi. Scale bar: 50μm

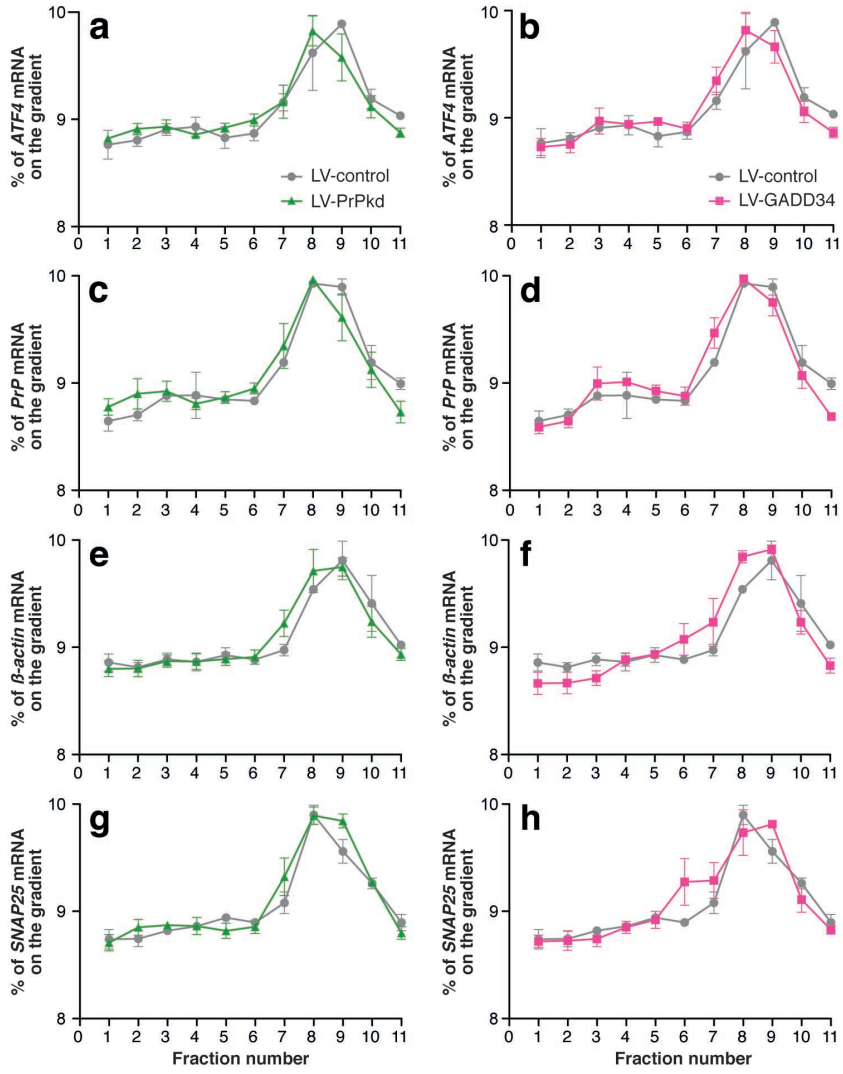

Figure S4. Quantification of specific mRNAs in individual fractions from polysomal gradients from hippocampi of LV-shPrP and LV-GADD34 treated prion-infected mice confirm reversal of activation of eIFα-P transational repression. mRNAs were quantitated in Northern blots on individual polysomal fractions from prion-infected LV-shPrP treated (green) or LV-GADD34 treated (pink), compared to LV-control treated (grey) controls, **a – h**. A shift in the peak of the curve to the right, as for *SNAP25*, is due to highest proportion of this mRNA occurring in a higher fraction where it is associated with more ribosomes, signifying a large increase in translation of these proteins in treated mice compared to LV-control treated controls at 9wpi, consistent with eIF2α-P repression. A shift in the peak of the curve to the left, as for *ATF4,* is due to the highest proportion of the mRNA being found in a lower fraction, where it is associated with fewer ribosomes, signifying a large decrease in translation, also consistent with inhibition of eIF2α-P, which normally induces ATF4. Thus preventing eIF2α-P formation by LV-shPrP (a,c,e,g) or driving its dephosphorylation via GADD34 over-expression (b,d,f,h) similarly affect translation. For all experiments n = 3 mice. Data in bar charts represents mean ± s.e.m.

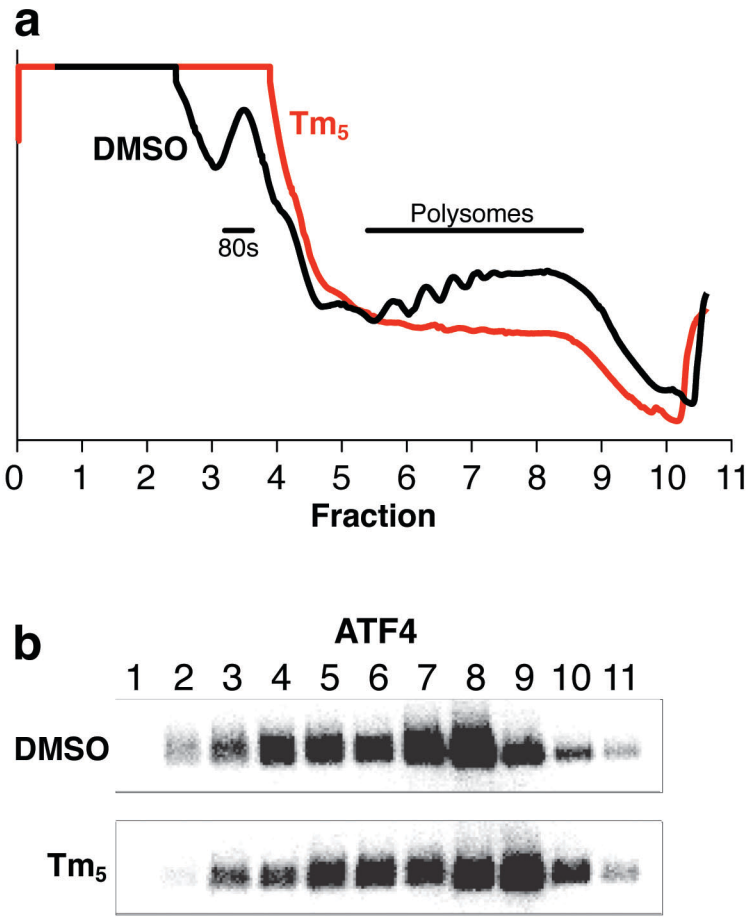

Figure S5. Tunicamycin, an ER stressor, induces eIF2α–P-mediated changes in translation in HeLa cells. **a**, Polysomal profiles from HeLa cells treated with tunicamycin (Tm) (red) and from control cells treated with DMSO (black) show reduction in active polysomes (fractions 6-11) in Tm-treated cells. Thus the area under the Tm curve is lower than under the DMSO curve, representing reduced numbers of actively translating polysomes. This is consistent with translational repression by activation of eIF2α-P by Tm. In contrast, eIF2α-P induces ATF4, which is resistant to translational repression. **b**, Northern blots for *ATF4* mRNA in individual polysomal fractions from Tm treated cells show that proportionately more *ATF4* mRNA is in factions 9 and 10 after Tm treatment for 5 hours, compared to the majority being in fractions 7 and 8 after DMSO treatment. In each successive fraction the mRNA is associated with 5-8 more ribosomes, representing a large increase in translation when mRNA is more represented in the higher fractions. n=3; Northern blots were repeated in triplicate.

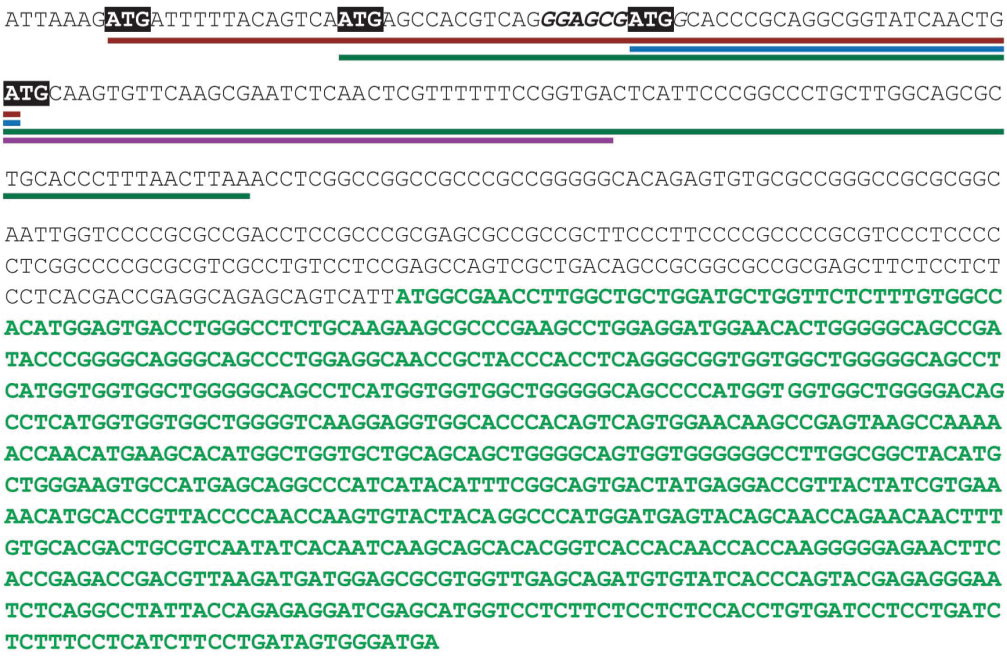

Figure S6. The human PrP gene has four upstream open reading frames (uORFs) in its 5' UTR, which may prevent translational repression of PrP by high levels of eIF2α-P. ATGs (highlighted) and the resultant uORFs are shown for each one (solid coloured lines). 5' UTR sequence is in black, coding sequence is shown in green. eIF2α phosphorylation determines the concentration of ternary complex and consequently the rate of translation initiation. When eIF2α-P levels are low, ternary complex concentration is high and normal mRNA transcripts with short 5' UTRs are translated with high efficiency. However, transcripts like *ATF4*[1,2], *BACE1*[3] and *PrP* (above) with long, uORF-containing, secondary structure-rich 5' UTRs are inefficiently translated. When eIF2α-P levels are high, under ER stress conditions, the translation of normal mRNA transcripts is inhibited as for SNAP25, PSD95, β actin, while transcripts with long, uORF-containing, structured 5' UTRs are well known to be translated with increased efficiency (de-repression) under these conditions. See Sonenberg and Hinnebusch, Cell, 2009 for review[4].

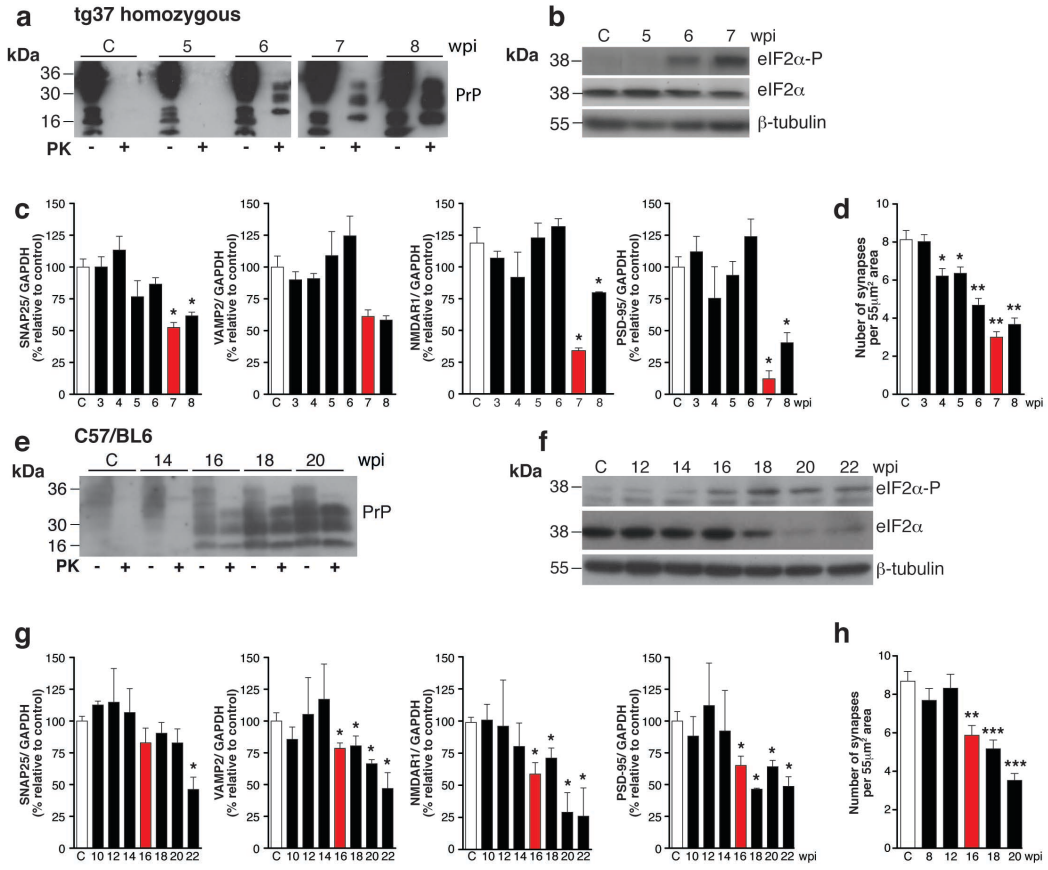

Figure S7. Onset of eIF2α phosphorylation and eIF2α-P-mediated translational repression correlates with levels of PrP in different lines of mice. a-d: Homozygous tg37 mice, in which mouse PrP is expressed at ~6x wild type levels. **a**, Levels of total PrP rise during disease and protease resistant PrP^{Sc} is first detected at 6wpi. **b**, eIF2α-P is first detected at 6wpi, and **c**, levels of synaptic proteins SNAP25, VAMP2, NMDAR1 and PSD-95 decrease abruptly and significantly after 6wpi. **d**, Synapse number declines from 4wpi and further decreases after 6wpi. Mice die at 8wpi. **e-h:** C57/Bl6 mice, that express PrP at 1x wild type levels. **e**, Levels of total PrP rise during disease and protease resistant PrP^{Sc} is first detected at 16wpi. **f**, eIF2α-P is detected at 16wpi when synaptic protein levels decline significantly, **g**, as does synapse number, **h**. For all experiments n = 3 mice, data in bar charts represents mean ± s.e.m. One-way ANOVA with Tukey's post test was used for multiple comparisons; $p < 0.05$*; $p < 0.005$**, $p < 0.0001$***. Control mice were injected with normal brain homogenate (NBH) and examined at each time point. Data from all control groups was averaged to simplify figures for western blots. Representative blots and EM bar charts are control samples from 8wpi for homozygous mice and 22wpi for C57/Bl6 mice.

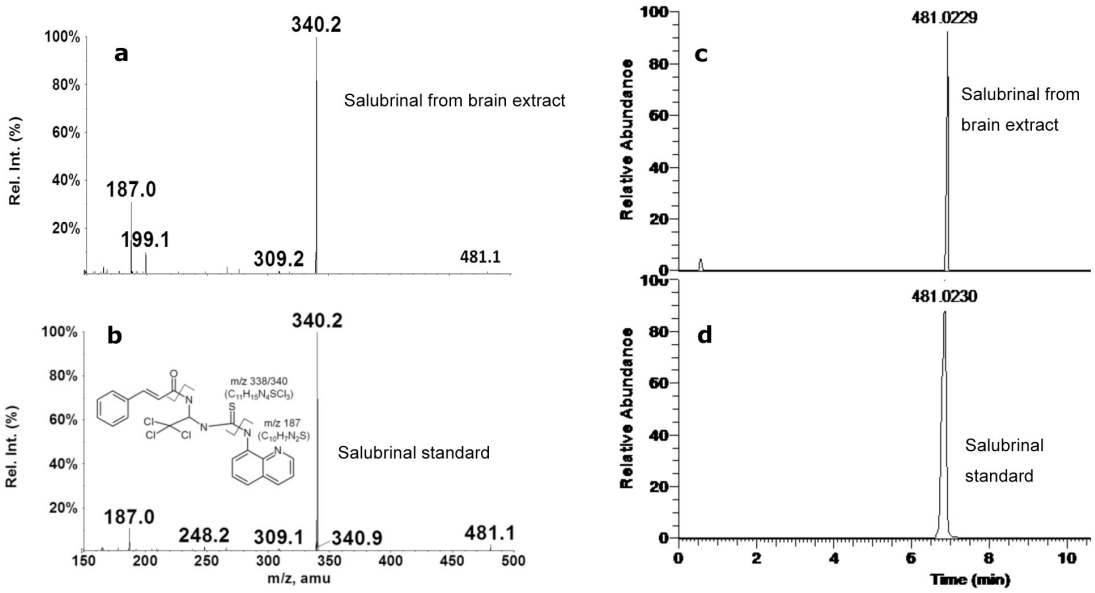

Figure S8. LC-MS confirmation of salubrinal in mouse brain tissue following interperitoneal administration. The MS product ion spectrum of the salubrinal extracted from mouse brain tissue **a**, matched with that of authentic salubrinal **b**, providing confirmation of the presence of saubrinal in mouse brain. LC-MS extracted ion chromatogram confirmed the presence of the salubrinal $[M+H]^+$ ions in mouse brain extract 2 hours after salubrinal administration **c**, and this matched with the retention time and exact mass of a salubrinal standard analysed under the same conditions **d**. The two main chlorine isotopes of salubrinal were confirmed in brain: theoretical *m/z* 479.0261 and *m/z* 481.0232, found *m/z* 479.0251 (2 ppm) and *m/z* 481.0229 (0.6 ppm), respectively, with matching of all the main isotope peaks with standard salubrinal. Measured salubrinal concentrations at 2 hours after administration were 9.5 ± 1.9 pmol/g (wet weight) in brain tissue and 18 ± 2.8 nmol/L in blood plasma. Less than 1 pmol/g of salubrinal was detectable at 24 hours in mouse brain or plasma.

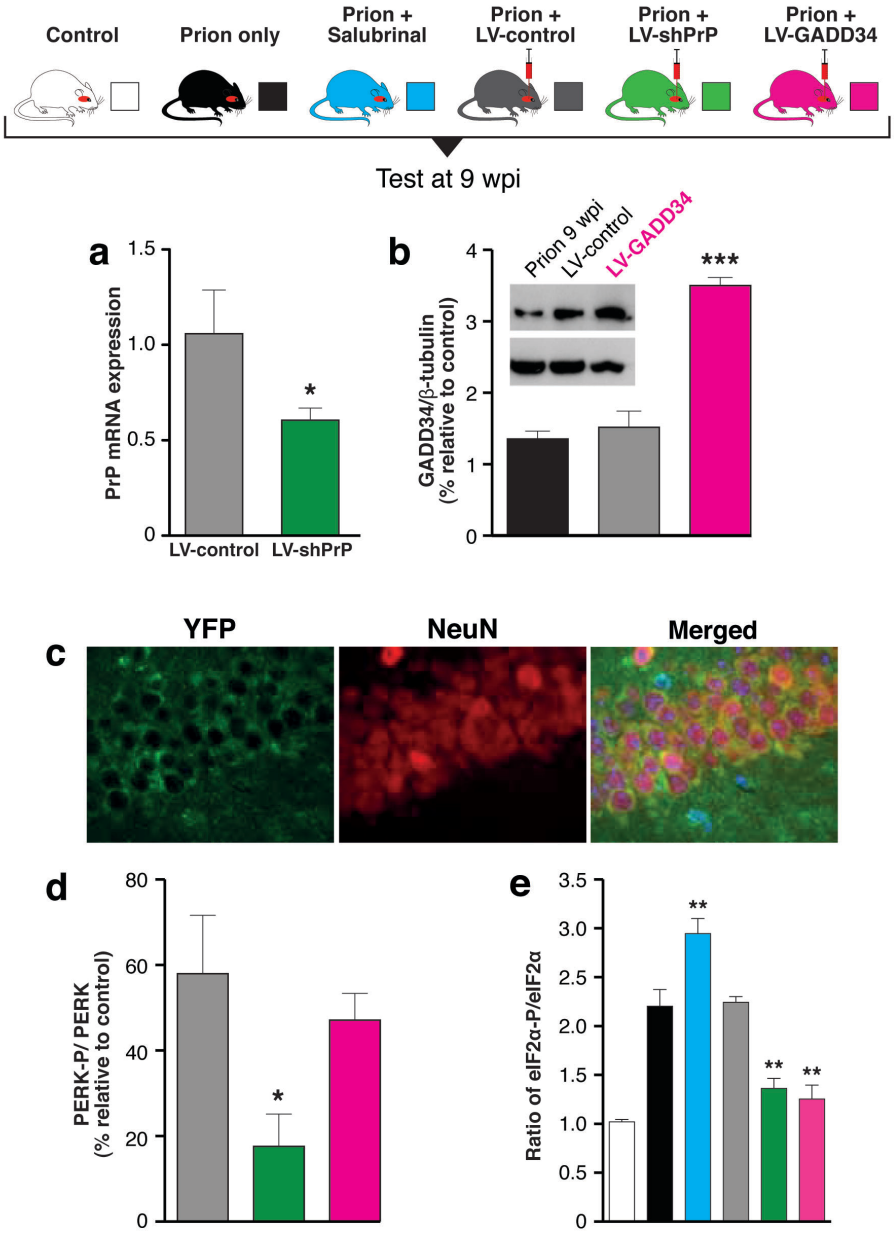

Figure S9. Confirmation of neuronal viral expression and quantification of PERK-P and eIF2α-P in prion-infected mice. a, qPCR on RNA from whole hippocampi of LV-shPrP treated mice confirms knockdown of ~50% of PrP mRNA 3 weeks after LV-shPrP injection. **b,** LV-GADD34 expression is confirmed in hippocampi 3 weeks after LV-GADD34 injection by western blot for GADD34 and quantification (bar chart). **c,** Neuronal expression is confirmed by in CA1 neurons by immunostaining for virally-expressed YFP (green) and the neuronal marker, NeuN (red). **d**, LV-shPrP reduces PERK-P in prion-infected mice. **e**, Both LV-shPrP and LV-GADD34 reduce eIF2α-P levels in prion infected mice, while salubrinal treatment increases this. For all experiments n = 3 mice. Data in bar charts represents mean ± s.e.m. One-way ANOVA with Tukey's post test was used for multiple comparisons; p <0.05*; p <0.005**, p <0.0001***. Control mice were injected with normal brain homogenate (NBH) and taken at 9wpi time point.

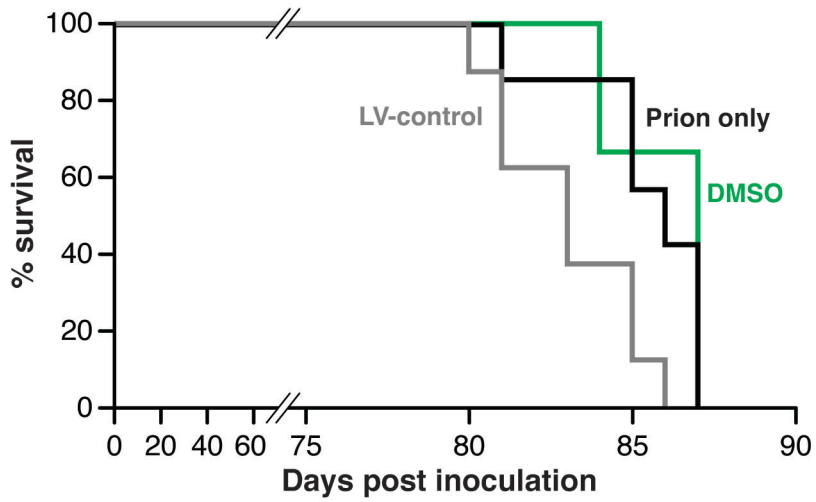

Figure S10. Kaplan Meier survival plots for prion infected control mice
Survival in LV-control treated (controls for LV-shPrP and LV-GADD34) and DMSO treated mice (controls for salubrinal treatment) is not significantly different from that of prion-only control mice.

Supplementary Methods

Real-time PCR. RNA was extracted from hippocampi using the mirVANA RNA/miRNA isolation kit (Ambion, Inc), mRNA was reversed transcribed and semi-quantative real-time PCR performed using sybr green supermix (Applied Biosystems). The following primers from mouse PrP, ATF4, CHOP, SNAP25 and ribosomal protein-144 coding sequences were used:
(PrP) 5'- GAGCCAAGCAGACTATCAGTC -3'(forward), 5'-TCAGTCCACATAGTCACAAAGAG -3'(reverse);
(Rp144) 5'- GGCCGGTCTCTCGTTCTCA-3' (forward), 5'-TTACAGAAAGTCCTTCGGGTTTTT-3' (reverse);
(ATF4) 5'- TCGATGCTCTGTTTCGAATGG -3' (forward), 5'-CCAACGTGGTCAAGAGCTCAT-3' (reverse);
(CHOP) 5'- CACACGCACATCCCAAAGC -3' (forward), 5'-CCTGGGCCATAGAACTCTGACT -3' (reverse);
(SNAP25) 5'- GGCTGACCAGCTGGCTGAT-3' (forward) 5'-TGCCAGCATCTTTACTCTCTTCAA -3' (reverse);
(VAMP2) 5'- GCTGGATGACCGTGCAGAT -3' (forward) 5'-TGGCTGCACTTGTTTCAAACTG-3' (reverse);
(PSD-95) 5'- AGTCTGTGCGAGAGGTAG-3' (forward) 5'-GGATGAAGATGGCGATAGG-3' (reverse);
(NMDAR1) 5'-CGCGAGATCTCTGGGAAT -3' (forward) 5'-GACTCGTTCTTGCCGTTGATTA-3' (reverse).
Fold difference was analysed comparing either control (NBH) to prion samples or LV-control to LV-shPrP samples using the comparative Ct method.

ER stress of HeLa cells. HeLa cells were treated with 2.5μg/ml tunicamycin for 0, 2, 5 or 10 hours and used as a positive control for ER stress for polysomal fraction analysis and immunoblots of the UPR pathway.

LC-Mass Spectrometry for analysis of salubrinal in brain tissue. Mice were injected with 1 mg/kg of salubrinal, control mice with diluted DMSO in saline (n=5 each group). After 2 and 24 hours blood plasma and whole brains were taken. Samples (200 mg) were extracted with chloroform:methanol (2:1), the solvent

evaporated to dryness and the dry residue redissolved in methanol before analysis. Salubrinal quantitative analysis (using external standards) was by LC-MS/MS (Applied Biosystyems 4000 QTRAP) and acurate mass determination was by UPLC-MS (Thermo Scientific Orbitrap Exactive). LC conditions: 5µl injection volume, Agilent SB C18 column (2.1 x 100 mm) or C18 Synergy Hydro (150 x 3 mm), water to-acetonitrile gradient modified with 0.1% formic acid. LC-MS/MS multiple reaction monitoring used precursor–product ion pairs of *m/z* 479.2>187.1 and *m/z* 481.2>187.1 in positive electrospray ionisation mode (ES^+). Both isotopes were monitored. Accurate mass LC-MS used ES^+ mode, scan range *m/z* 100 to 1200, a resolution of 25,000, ions acquired with and without applying parameters to induce collisional dissociation.

Immunocytochemistry for GFP expression. Lentivirally injected brains were paraffin embedded and immunostained for yellow fluorescent protein (YFP) using primary antibody anti-GFP (1:500; Abcam) following antigen retrival with sodium citrate. Sections were then incubated with secondary antibody Alexa-fluor-488 (1:500; Invitrogen) to visualize cells expressing YFP. Images were captured using Zeiss 200M and colorbri camara (Zeiss).

Supplementary references

1 O'Connor, T. *et al.* Phosphorylation of the translation initiation factor eIF2alpha increases BACE1 levels and promotes amyloidogenesis. *Neuron* **60**, 988-1009, (2008).

2 Harding, H. P. *et al.* Regulated translation initiation controls stress-induced gene expression in mammalian cells. *Mol Cell* **6**, 1099-1108, (2000).

3 Spriggs, K. A., Bushell, M. & Willis, A. E. Translational regulation of gene expression during conditions of cell stress. *Mol Cell* **40**, 228-237,(2010).

4 Sonenberg, N and Hinnenbusch, A.G. Regulation of translation initiation in eukaryotes: mechanisms and biological targets. *Cell* 2009 136, 731-45 (2009).